A Permian–Triassic boundary section at Quinn River Crossing, northwestern Nevada, and implications for the cause of the Early Triassic chert gap on the western Pangean margin

Erik A. Sperling[†]
James C. Ingle, Jr.
Department of Geological and Environmental Sciences, Braun Hall, Building 320, Stanford University, Stanford, California 94305, USA

ABSTRACT

The Upper Permian–Lower Triassic Quinn River Formation in northwestern Nevada was previously thought to represent an incomplete Permian–Triassic boundary sequence, owing to an inferred disconformable relationship between Permian radiolarian- and spicule-rich chert and overlying Triassic siltstone. Petrographic and geochemical studies demonstrate that the "siltstone" is in fact a radiolarian-bearing early authigenic dolomicrite, with both the chert and dolomicrite deposited conformably in deep water. Chert production declined or ceased in the Late Permian and reappeared in the Spathian, forming a widespread "chert gap" in Permian–Triassic sequences. Given the conformable lithofacies relationships, deep-water depositional setting, new radiolarian data extending ranges of key taxa, and the presence of the global chert gap, sedimentation in the Quinn River Formation was apparently continuous across the Permian–Triassic boundary. This represents the first Permian–Triassic boundary section in the United States portion of the North American Cordillera, and one of the few deep-water sections worldwide. Organic carbon isotope stratigraphy of the Quinn River Formation displays multiple excursions through sediments of Wuchiapingian–Anisian age, with a negative excursion 1.54 m above the chert-shale transition likely representing the Permian–Triassic boundary.

The multiple excursions in the organic carbon record verify studies of the carbonate carbon record in China that suggest instability in the isotopic record throughout the Early Triassic, and demonstrate that the Permian–Triassic boundary isotope excursion was not an isolated event. Stratigraphic variation in redox-sensitive trace metals indicates that seawater became less oxic slightly before the chert-shale transition, in turn impacting siliceous sponge communities and creating the widespread chert gap. The distinctive dolomicrites in the Quinn River Formation represent a widespread lithofacies deposited in many localities during the Late Permian–Early Triassic and express early authigenic formation of dolomite via microbial sulfate reduction in organic-rich, low-oxygen environments.

Keywords: Permian–Triassic mass extinction, Humboldt County, Nevada, chemostratigraphy, chert, anoxia.

INTRODUCTION

The Permian and Triassic Periods were some of the most interesting times in Earth history. This interval saw the final coalescence of the supercontinent of Pangea, a change from an icehouse to a greenhouse climatic state, large shifts in the oceanic isotope ratios of carbon, oxygen, sulfur, and strontium, and the greatest mass extinction of all time (Hein, 2004). The Permian–Triassic mass extinction was the most devastating in Earth history, with 80–96% of species becoming extinct (Raup and Sepkoski, 1982; Erwin et al., 2002). The causes, timing, and extent of the extinction are much debated, although study in the last 20 years has sharpened understanding. Possible killing mechanisms for the mass extinction, several of which might be related, include intense volcanism (Renne et al., 1995), global marine anoxia (Isozaki, 1997; Wignall and Twitchett, 2002), bolide impact (Kaiho et al., 2001; Becker et al., 2001), euxinia (Grice et al., 2005; Kump et al., 2005), and CO_2 poisoning (Knoll et al., 1996), among many others (see reviews in Erwin et al., 2002; Benton and Twitchett, 2003). In North America, the Permian–Triassic record has traditionally been regarded as unconformable (e.g., Collinson et al., 1976), and the apparent lack of data from the western Pangean margin has in part hindered understanding of the mass extinction. However, the discovery of complete Permian–Triassic sections in the Canadian Rockies (Henderson, 1997), in sections previously believed unconformable, lends credence to the possibility of complete sections in the American portion of the Cordillera (Alvarez and O'Connor, 2002).

This paper presents evidence from the Quinn River Formation, exposed in the Bilk Creek Mountains of northwestern Nevada, suggesting that it contains one of the first documented Permian–Triassic boundary sections in the western United States. Given the rapidity of this extinction (Bowring et al., 1998), new boundary sections must be carefully scrutinized for possible hiatuses or unconformities. This study investigates the lithostratigraphic, biostratigraphic, and chemostratigraphic (particularly organic carbon isotope) evidence from the Quinn River Formation in an attempt to establish the stratigraphic position and fidelity of the Permian–Triassic sequence. The nature of redox trends through this critical period in Earth history was also studied through facies analysis and trace metal proxies. The Quinn River Formation shows many similarities to other Permian–Triassic sections, especially those in the Canadian Cordillera (Henderson, 1997) and accreted deep-sea cherts in Japan (Isozaki, 1997). Specifically, the Quinn River Formation contains evidence of the near-global "chert gap" that strongly affected both the western Pangean margin (Beauchamp and Baud, 2002) and many (but not all—see Takemura et al., 2003) deep-water sections worldwide (Isozaki, 1997). Comparisons of

[†]Present address: Department of Geology and Geophysics, Yale University, P.O. Box 208109, New Haven, Connecticut 06520, USA; e-mail: erik.sperling@yale.edu.

GSA Bulletin; May/June 2006; v. 118; no. 5/6; p. 733–746; doi: 10.1130/B25803.1; 7 figures; 2 tables; Data Repository item 2006096.

these localities help to explain the nature of Permian–Triassic oceanographic changes and their effect on the stratigraphic record.

GEOLOGIC SETTING

During the Permian–Triassic transition, the Cordilleran region of North America was divided into several distinct north-south–trending provinces: the craton; the westward-deepening miogeocline; the allochthonous slope, rise, and basin floor of the Golconda Allochthon; and the McCloud-affinity fringing volcanic arc system (Miller et al., 1992). The Quinn River sediments analyzed in this study were deposited in a deep-water offshore setting adjacent to the McCloud-affinity arc system. The Quinn River Formation makes up part of the so-called Black Rock Terrane, which in turn is one of the terranes representing the McCloud arc (Miller, 1987). The Quinn River sediments were accreted to the continent during post–Middle Triassic time and were subsequently exposed in the Bilk Creek Mountains of northwestern Nevada during Tertiary Basin and Range extension.

The Quinn River Formation is exposed within the U.S. Geological Survey Mustang Spring quadrangle map, ~60 mi northwest of Winnemucca, Nevada (see Fig. 1). The site is accessible by dirt roads and easily seen from State Highway 140 (Fig. 2). A geologic map of the area, showing the line of section used in this study, can be found in Jones (1990).

PREVIOUS STUDIES

The Quinn River Formation has, despite its limited outcrop, been the subject of numerous studies. The structural significance of the section was first noticed by Willden (1961), who recognized the post–Middle Triassic Quinn River Thrust, which places Permian and Triassic strata over Mesozoic volcanics.

Regional stratigraphic relations have been discussed by Skinner and Wilde (1966), Ketner and Wardlaw (1981), Silberling and Jones (1982), Jones (1990), and Blome and Reed (1995). Skinner and Wilde (1966) recognized that the Early Permian fusulinids in the Permian limestone at Quinn River were identical to the McCloud Limestone fauna in the Eastern Klamath Terrane 300 km to the east. This observation was confirmed by Silberling and Jones (1982), who reported radiolarians and mollusks in the Quinn River Formation that allowed for additional correlation with the Eastern Klamath Terrane. Ketner and Wardlaw (1981) correlated the Quinn River Formation with the allochthonous and parautochthonous rocks of the Farrel Canyon, Edna Mountain, Adam Peak, and Antler Peak Formations in the Osgood Mountains area east of the Quinn River section. More recent stratigraphic and paleontologic studies by Jones (1990) and Blome and Reed (1995) suggest closer ties with the Eastern Klamath Terrane and other terranes of the McCloud fringing arc system to the west (e.g., Miller, 1987), as opposed to rocks within the Golconda Allochthon to the east.

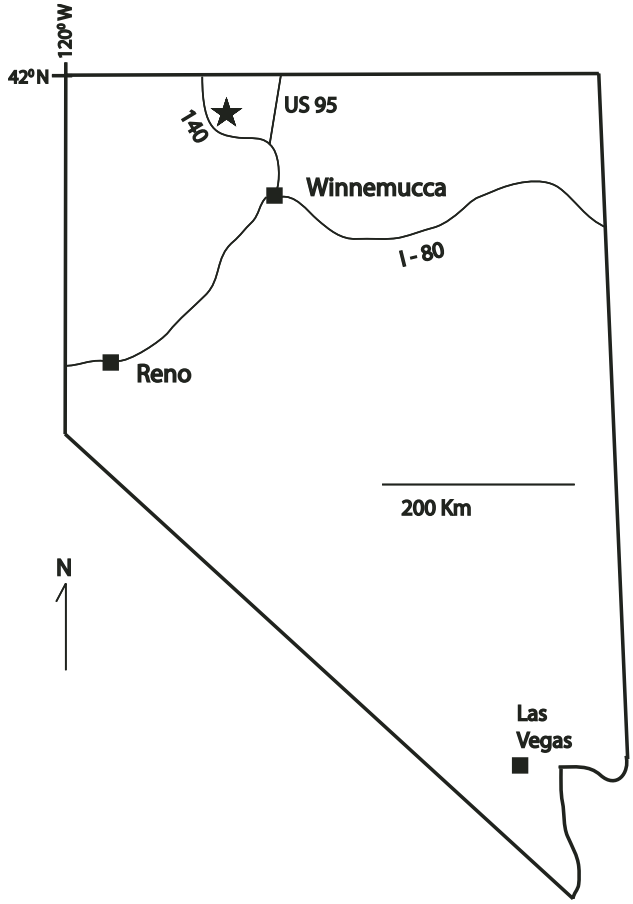

Figure 1. Map of Nevada, with a star showing the location of the measured section through the Permian–Triassic Quinn River Formation, analyzed in this report at Quinn River Crossing, Humboldt County, Nevada.

LITHOSTRATIGRAPHY

Stratigraphy of the Bilk Creek Mountains

The relevant pre-Tertiary stratigraphy of the Bilk Creek Mountains consists of three units: the Permian Bilk Creek Limestone, an unnamed Permian volcaniclastic unit, and the Permian–Triassic Quinn River Formation. These rocks are on the upper plate of the Quinn River Thrust, which places upper Paleozoic units over a Mesozoic volcanic sequence dated at 191 ± 9 Ma (Jones, 1990). The Bilk Creek Limestone consists of ~600 m of cherty, fossiliferous gray limestone. It is overlain by the 125-m-thick Permian volcaniclastic unit, which includes beds of spiculitic and tuffaceous argillite, turbiditic volcaniclastic sandstones, siltstones, and mudstones (Jones, 1990). These beds strike at a slightly oblique angle into the Quinn River Formation, indicating a fault contact or an angular unconformity.

Because similar rock types occur multiple times within the Quinn River Formation, it was broken into six distinct units to better simplify descriptions. These units, in ascending stratigraphic order, are:

Unit 1. The basal lithology of the Quinn River Formation consists of a pale-green, fine-grained siliceous tuff. A 2-m-thick brown, silicified, bioclastic calcirudite sits above the tuff, forms an obvious landmark that can be seen from the highway, and represents the base of the measured section in this study (see Fig. 3).

Unit 2. Fifteen meters of light-brown dolomite.

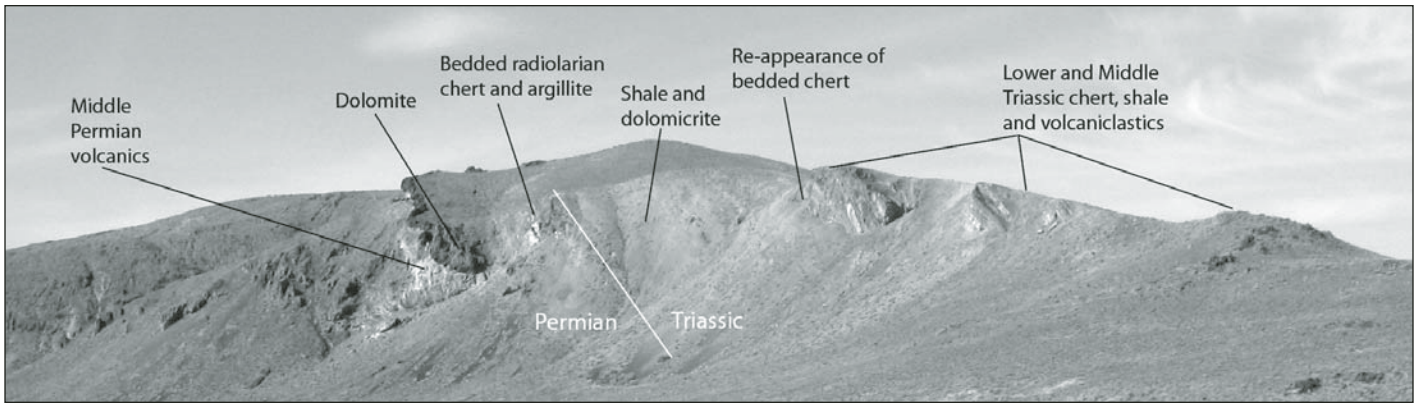

Figure 2. Annotated outcrop-scale view of the Quinn River Formation exposed adjacent to State Highway 140 at Quinn River Crossing, Nevada. The annotated units encompass ~180 m of section.

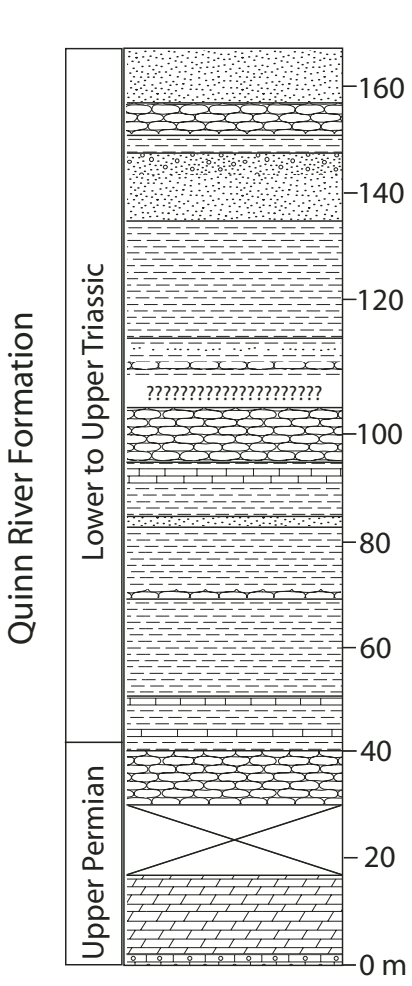

Unit	Lithology	Key fossils
6	White and grey volcaniclastic ss Interbedded chert and shale Coarse sand to granule conglomerate w/ interbeds of chert, shale, volcaniclastics Dominantly shale w/ minor chert, tuffaceous material and fossiliferous limestone turbidite Section moved to J120 marker	Ladinian to Carnian radiolarians and conodonts (Blome and Reed, 1995; Jones, 1990) Late Spathian to early Anisian ammonite (Jones, 1990)
5	Interbedded chert and very dark shale, some tuffaceous strata	Spathian-Anisian radiolarians (Blome and Reed, 1995)
4	Meter-thick interbeds of shale and massive brown dolomicrite Brown volcaniclastic sandstone Dominantly shale Thin cherty mudstone with spheroids Dominantly shale Interbeds of laminated, brown-weathering dolomicrite and shale	Spathian-Anisian radiolarians (Blome and Reed, 1995) Earliest Triassic radiolarians (Jones, 1990)
3	Bedded radiolarian and spiculitic chert and argillite with some ash deposits	Wuchiapingian and Changhsingian radiolarians (Blome and Reed,1995)
2	Light brown dolomite	Wordian brachiopods (Ketner and Wardlaw, 1981)
1	Bioclastic calcirudite (base of measured section) 15 meters of cherty tuff (not shown)	

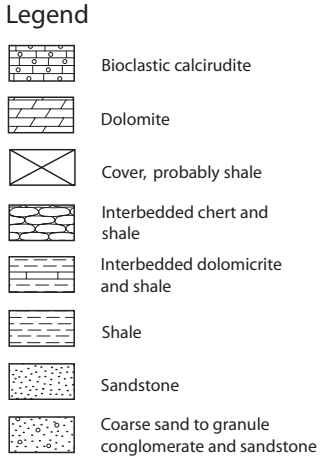

Figure 3. Thickness and lithologic subunits of the Quinn River Formation exposed at Quinn River Crossing, Nevada (this study), with key biostratigraphic data from previous studies. Question marks in the lithologic column indicate truncated strata.

Unit 3. Twenty-five meters of interbedded gray to black radiolarian and spiculitic chert and argillite.

Unit 4. This 60-m-thick package consists predominantly of interbedded dark laminated dolomicrite and shale. The dolomicrites were misidentified in the field by previous authors as siltstones. Petrographic and geochemical studies have demonstrated that they are early authigenic deep-water dolomites. The middle of unit 4 contains a single 2-m-thick cherty mudstone with siliceous "spheroids" and possible sponge spicules. This thin chert is succeeded by meter-thick interbeds of shale and massive brown dolomicrite, as well as minor chert and brown volcaniclastic sandstone.

Unit 5. Ten meters of interbedded chert and very dark shale, with a few tuffaceous interbeds. The top of unit 5 contains an intensely folded section with truncated beds.

Unit 6. This unit begins after the folded interval noted above; is a heterogeneous mix of chert, shale, volcaniclastics, and tuffaceous sediments; and continues to the point at which the section is covered by Tertiary volcanics. No dolomicrites were identified in this unit. Unit 6 also contains strong evidence of deep-water gravity-flow deposits, including a limestone turbidite, a strata-bound slumped sandstone bed, and ~5 m of coarse sand-conglomerate with muddy rip-up clasts. Rock types are commonly gradational, and it is difficult to easily distinguish the multiple fine-grained lithologies. This unit is ~60–65 m thick.

The upper part of the Quinn River section contains several intervals with tight folds that probably represent drag folds from thrust faults developed during Mesozoic tectonism. However, the critical Permian–Triassic boundary interval does not appear to be affected by faulting. The first probable fault appears at ~82 m in Figure 3. The position of the truncated strata is indicated in the stratigraphic column by question marks.

Detailed Stratigraphy of the Quinn River Formation

In addition to the formation-scale measured section (Fig. 3), 8 m of section spanning the unit 3–unit 4 contact was logged at a centimeter scale (Fig. 4). The contact between the Permian chert and the overlying units was considered a paraconformity by previous authors because of the sharp contact between the chert and siltstone. This contact, together with a lack of diagnostic Early Triassic fossils, was cited as the main reason for regarding the section as incomplete. To determine the nature of this lithologic change, thin-section petrography and bulk-rock geochemistry were used to study the boundary interval and to divide the rocks into six facies that are described lithologically in Table 1 and geochemically in Table 2. Thin-section photomicrographs that illustrate these facies are contained in Supplemental Figures DR1–DR12 in the GSA Data Repository[1]. Figure 4 shows the stratigraphic log of the boundary interval together with the positions of samples used in the petrographic and geochemical studies. Thin calcite crystals occur at the base of several dolomicrite beds, including the chert-dolomicrite contact. The prevalence of bed-parallel calcite crystals was noted in a regional study by McDaniel (1982); the fragile crystals are likely diagenetic in origin, resulting from calcite filling cracks developed during tectonism.

AGE OF THE QUINN RIVER FORMATION

Previous Biostratigraphic Studies

Three studies focused on the biostratigraphy of the Quinn River Formation (Ketner and Wardlaw, 1981; Jones, 1990; Blome and Reed, 1995). Ketner and Wardlaw (1981) reported the brachiopods *Ctenalosia fixata* and *Stenocisma* sp., indicative of a Wordian age (Blome and Reed, 1995), from the unit 2 dolomite near the base of the section. Ketner and Wardlaw (1981) also reported a late Middle Triassic pelecypod and ammonite fauna in beds several meters above the Permian chert. However, Blome and Reed (1995) note that in a written communication, N.J. Silberling (in 1993) indicated that the late Middle Triassic (Ladinian) pectenacids *(Daonella, Posidonia)* and the ammonite *Protrachyceras* were actually collected from the middle part of the volcaniclastic sequence (most likely unit 6 of this report) as opposed to directly above the Permian chert.

The Permian chert (unit 3) has been the subject of several studies. Jones (1990) studied radiolarians from this unit and assigned a Guadalupian age. However, more recent studies have failed to recover the follicucullids used to make this age assignment (Blome and Reed, 1995), and Jones independently determined that they were not present in her samples, thus suggesting a post-Guadalupian age for the chert. In a more detailed study, Blome and Reed (1995) recovered *Albaillella levis* and *A.* sp. cf. *A. triangularis* from the lower half of the Permian chert, *Triplanospongos* sp. cf. *T. dekkasensis* throughout the unit, and *Neoalbaillella* sp. aff. *N. ornithoformis* ~3 m below the top of the unit. On the basis of this fauna, Blome and Reed (1995) assigned an Abadehian to Djulfian age (≈Wuchiapingian, according to Gradstein et al., 2004) to unit 3. The significance of their radiolarian data in light of new zonations is discussed in the following paragraphs. Citing the lack of any pre-Wuchiapingian fossils between the Wordian brachiopods in unit 2 and the first appearance of *Triplanospongos* in unit 3, Blome and Reed (1995) concluded that the lithologic change between units 2 and 3 represents a disconformity where Capitanian strata are missing. Jones (1990) recovered several Wordian conodont elements near the top of the unit 3 chert, but because they occur above a well-developed Lopingian radiolarian fauna, Blome and Reed (1995) considered them reworked.

Whereas Permian fossils in the Quinn River Formation have been studied in detail, few fossils have been found in the upper part of the formation. On the basis of the pelecypods and ammonite mentioned previously, the upper part of the Quinn River Formation has long been considered Middle to Upper Triassic. Silberling and Jones (1982) found "primitive Triassic radiolarians" from the clastic unit, whereas Jones (1990) reported earliest Triassic radiolarians 82 m above the base of the formation. She also reported a late Spathian to early Anisian ammonite (an "acrochordiceratid" in Jones, 1990, p. 251 = *Paracrochordiceras* Spath, late early Anisian, Hugo Bucher, Université de Lausanne, 1992, written commun. to Blome and Reed) from the same locality. Near the top of the section, Jones (1990) reported Middle Triassic radiolarians and the Ladinian(?) conodont *Neogondolella* sp. cf. *N. constricta*.

Gradational rock types and apparent differences in measuring across faults/folds make it difficult to precisely correlate between the three detailed stratigraphic columns (Jones, 1990; Blome and Reed, 1995; this study) that have been produced. Consequently, it is difficult to determine the exact horizon from which the *Paracrochordiceras* was recovered. On the basis of comparison of stratigraphic thicknesses reported in the Jones (1990) paper, her field notes, and her painted "J120" mark seen in the field, the ammonite was probably found near the sand-to-granule beds in unit 6, at ~135 m in Figure 3.

Despite a thorough study, Blome and Reed (1995) were unable to recover many useful radiolarian specimens from the upper part of the Quinn River Formation, with only 4 of 27 samples yielding identifiable specimens. From samples several meters below the unit 5 chert, and also in the middle of that unit, they report

[1]GSA Data Repository item 2006096, stable isotope, total organic carbon and bulk-rock geochemical data contained in Tables DR1 and DR2, is available on the Web at http://www.geosociety.org/pubs/ft2006.htm. Requests may also be sent to editing@geosociety.org.

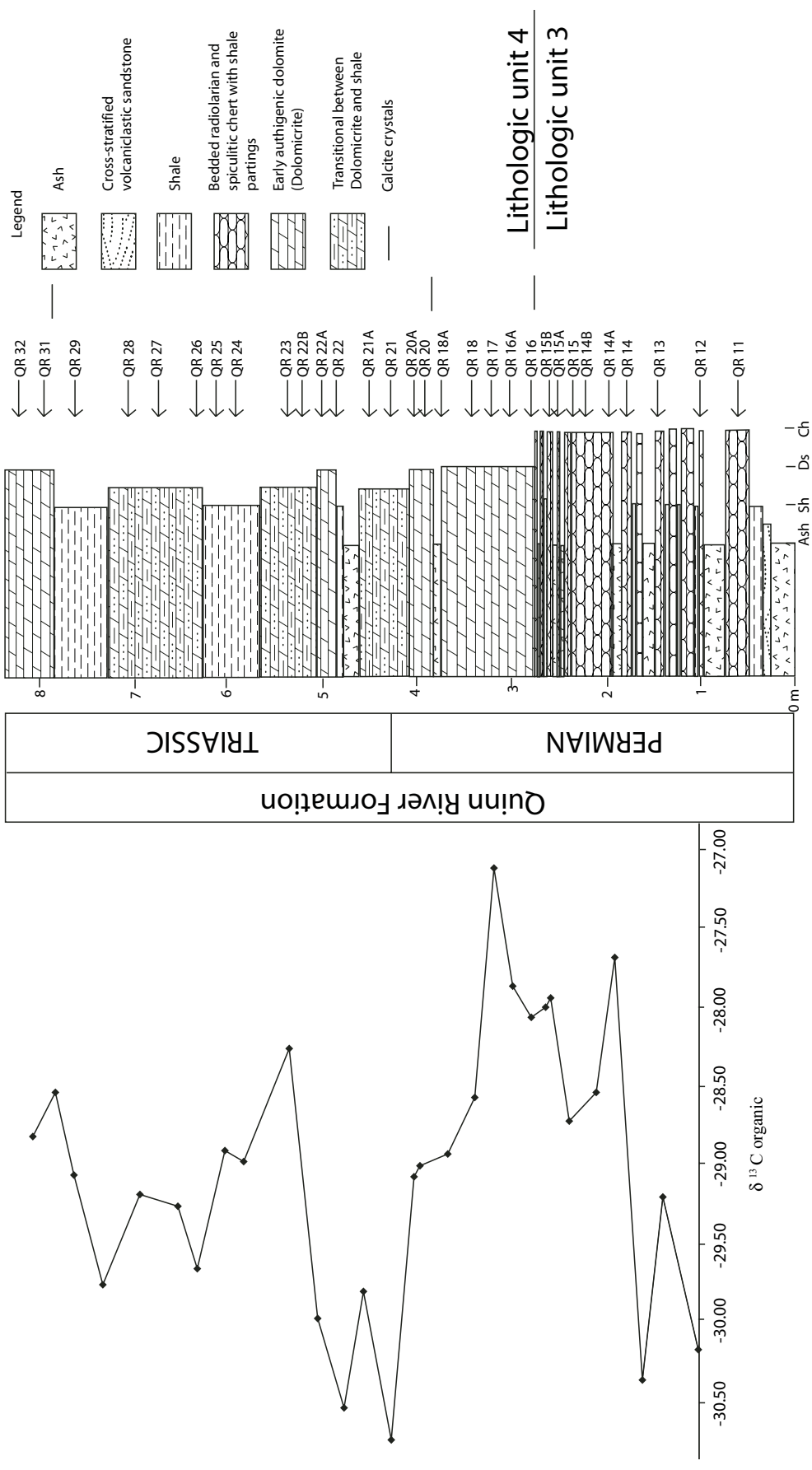

Figure 4. Detailed lithostratigraphy of the Permian–Triassic boundary interval in the Quinn River Formation at Quinn River Crossing, Nevada, with sample localities and organic carbon isotope stratigraphy. The measured section starts 275 cm below the contact between lithologic units 3 and 4 (chert-dolomicrite contact). Permian–Triassic boundary is defined isotopically and therefore does not correspond directly to the biostratigraphic boundary but to a level high in the Changhsingian and near the mass extinction horizon (see discussion in text). Note organic carbon curve at left. Sh—shale; Ch—chert; Ds—dolomicrite.

poorly preserved, recrystallized forms from two of their samples (DR-1126 and -1128) that strongly resemble Early Triassic and early Middle Triassic (Anisian) nodose forms assignable to the entactiniid genus *Cryptostephanidium*. They also note that several of the Quinn River specimens resemble *Cryptostephanidium longispinosum* and *Cryptostephanidium* sp. cf. *C. verrucosum* taxa. These two forms range through the Lower Triassic and lower Anisian *Parentactinia nakatsugawaensis* and *Hozmadia gifuensis* Zones of Sugiyama (1992). Blome and Reed (1995) also recovered specimens 21 m below the top of the section that are indicative of a middle Carnian age.

Although the available radiolarian data in the Quinn River Formation are highly useful, Late Permian and Early Triassic radiolarian biostratigraphy is evolving rapidly. The near-global chert gap associated with Permian–Triassic boundary strata (Beauchamp and Baud, 2002), the almost total extinction of radiolarians in this interval (Kozur, 1998), and the lack of stratigraphically intact sections (Blome and Reed, 1992) have limited the resolution of radiolarian ranges needed to constrain the zonations. It is only recently that radiolarian-rich sections have been discovered that incorporate the Permian–Triassic boundary.

Review of New Radiolarian Zonations and Their Implications

At the time of publication, Beauchamp and Baud (2002) thought the chert gap was global in extent, but they now recognize that rare chert-rich successions are being discovered that cross the Permian–Triassic boundary (A. Baud, 2004, personal commun.). A complete chert succession has recently been found in New Zealand (Takemura et al., 2003), and siliceous mudstones that cross this boundary in Japan, China, and Thailand have allowed a revision of the zonations used by Blome and Reed (1995) to constrain the Quinn River Permian chert as pre-Changhsingian. Most notably, the ranges of many taxa have now been extended into the latest Changhsingian. Species from the Quinn River Formation such as *Triplanospongos dekkasensis, Ishigaum obesum, Nazarovella gracilis,* and *Hegleria mammilla* all range very close to the top of the Permian (Yao and Kuwahara, 2000; Sashida et al., 2000; Feng and Gu, 2002).

Kuwahara et al. (1998) erected four zones for the Upper Permian on the basis of assemblages in bedded chert of the Mino Belt of Southwest Japan. They are, in ascending order, the *Follicucullus scholasticus–F. ventricosus* Zone, the *F. charveti–Albaillella yamakitai* Zone, the *Neoalbaillella ornithoformis* Zone, and the *N. optima* Zone. These four zones approximately correspond to the lower and upper Wuchiapingian, and the lower and upper Changhsingian (Kuwahara et al., 1998; Yao and Kuwahara, 2000).

Kuwahara et al. (1998) confirm the suggestion by Sashida (1997) that the *N. optima* Zone is actually above the *N. ornithoformis* Zone, not below it as originally suggested by Ishiga (1986). On the basis of their new zonation, Kuwahara et al. (1998) suggest that the *F. charveti–Albaillella yamakitai* Assemblage Zone, which they date as early Late Permian, "may be correlative with the strata which yield *'A. triangularis'* and '*A.* sp. cf. *A. triangularis*' without neoalbaillellids in the Quinn River Formation (Blome and Reed, 1995)" (p. 397). This would suggest that the uppermost unit 3 chert at Quinn River containing forms assignable to *N. ornithoformis* would correspond to the lower Changhsingian.

New Triassic "Radiolarian" Data

An additional "radiolarian zone" was identified in Quinn River sediments during this study—the so-called spheroid zone of Yao and Kuwahara (2000). Thin sections of the thin cherty bed in unit 4 show numerous siliceous spheres. These unidentifiable spheres are probably radiolarian "ghosts;" but like spheroids from the Ursula Creek section, British Columbia (Wignall and Newton, 2004), they lack any ornamentation. Although the recognition of spheroids in Griesbachian strata at Opal Creek, Alberta, during the course of this study questions their usefulness as a precise marker within the Lower Triassic, the spheroids apparently were widespread during this time period and have not been reported from Middle Triassic strata. With the recognition of this "biozone,"[2] it

TABLE 1. LITHOLOGIC DESCRIPTION OF FACIES SPANNING THE PERMIAN–TRIASSIC BOUNDARY IN THE QUINN RIVER FORMATION, NEVADA

Facies	Lithology	Description	Thickness (cm)
A	Ash	Volcanic ash beds with double-terminated quartz grains; weathers to white clay	1–25; 10
B	Volcaniclastic sand	9 cm bed 2.5 m below top of unit 3, directly above thick ash bed; cross-stratified	9
C	Bedded chert (QR-1–QR-15)	Abundant radiolarians and sponge spicules, but sponges disappear near top. Upper samples pyritic. Interbedded with light-gray, organic-poor shale partings 1–10 cm thick. Some current-oriented sponge spicules.	5–60; 20
C	Bedded chert (QR-15A,B,C)	Similar to lower cherts in hand sample, but geochemically grade into overlying shales and dolomicrites	2–4; 3
D	Dolomicrite	Dark, with fine, organic-rich laminae. Consists of masses of tiny dolomite rhombs, intergrown with organic matter, pyrite, rare detrital silt, probable radiolarian ghosts.	15–100; 40
E	Shale	Dark, organic-rich laminated pyritic shales; barely discernible radiolarian(?) ghosts	1–50; 30
F	Transitional	Resembles mudstone in outcrop, but more competent than shale and more fissile than dolomicrites. Weathers gray to light yellow. Difficult to discern geochemically.	2–100; 30

Note: Thickness reported as the range; average in centimeters.

TABLE 2. GEOCHEMICAL CHARACTERIZATION, REPORTED IN WEIGHT PERCENTAGES, OF FACIES SPANNING THE PERMIAN–TRIASSIC BOUNDARY IN THE QUINN RIVER FORMATION, NEVADA

Facies	SiO_2	Al_2O_3	MgO	CaO
A	Not determined			
B	Not determined			
C (QR1–QR15)	93–98	0.8–3.1	0	<0.5
C (QR-15A,B,C)	85–91	7.8–8.6	1	0–1.39
D	25–56	1.0–6	9.0–20	12.0–34
E	78–85	6.0–14	trace	trace
F	76–84	7.0 –12	<1.0	<1.0

[2]Although the "spheroid" zone may not represent a true biozone, it is used here as a distinct and apparently widespread lithostratigraphic unit. Thin-section photomicrographs of the "spheroids" are contained in GSA Data Repository Supplemental Figures.

is suggested that the proper method for partitioning the Quinn River Formation is not through extending known Middle Triassic fossils 100 m downward, but rather viewing the formation as an essentially complete, relatively slowly deposited succession. The fossil data form a coherent sequence in the Quinn River Formation as follows: late Wuchiapingian radiolarians in the base of unit 3, early Changhsingian radiolarians at 37 m, the unit 3–unit 4 chert gap lithologic transition at ~40 m, Early Triassic "spheroid" radiolarians at 70 m, Spathian–Anisian radiolarians at ~95 m, the late Spathian–early Anisian ammonite at ~135 m in unit 6, and Ladinian to Carnian radiolarians and conodonts at the top of the section. The radiolarian data of Blome and Reed (1995), reinterpreted in light of more recent zonations, are shown in Figure 5.

The lack of positively identified latest Changhsingian and earliest Triassic fossils, although limiting the usefulness of the section for intensive study of the Permian–Triassic boundary, does not invalidate the probability of a complete section nor lessen its usefulness in understanding long-term deep-water redox trends. This is similar to Permian–Triassic sections in Japan and Thailand, where chert deposition also ceased in the *Neoalbaillella* Zones and reappeared in the *P. nakatsugawaensis* Zone, and where the Permian–Triassic boundary is assigned indirectly between the known data points (Isozaki, 1997; Sashida et al., 2000).

QUINN RIVER CHEMOSTRATIGRAPHY

Laboratory Procedures

Organic carbon isotope stratigraphy was conducted at Quinn River in an attempt to determine the location of the Permian–Triassic and other stage-level boundaries. Samples were cleaned, and the most fresh-looking material was ground to a flour for isotopic analysis. This powder was then weighed into silver capsules and repeatedly acidified with sulfurous acid in a 60 °C oven until all carbonate was removed. Dolomicrites were acidified in petri dishes with sulfurous acid and dilute phosphoric acid to ensure total removal of dolomite. Total organic carbon (TOC) therefore was not calculated for these samples.

All samples were run on a Finnigan MAT Delta Plus coupled to a Carlo Erba NAL1500 Series II Elemental Analyzer. Eighty samples (plus nine replicates) were run for $\delta^{13}C$ (reported in standard notation relative to PDB standard), $\delta^{15}N$ (reported relative to air), and TOC (reported as weight percentages). The average separation of the nine replicates was $0.351^{0/00}$ for ^{13}C; the precision of the mass spectrometer, on the basis of repeated measurements of the USGS-24 and IAEA-N1 standards, was better than $0.15^{0/00}$.

Twenty-nine samples from the QRF were analyzed for 11 major and 25 trace element compositions by X-ray fluorescence (XRF) on a Philips PW2400 wavelength dispersive XRF spectrometer with light element capability at the University of California, Berkeley. The rock powder used for the XRF analysis was the same as that used for the organic carbon isotopes. An additional four samples from the Ursula Creek Permian–Triassic section in British Columbia, provided by Tyler Beatty of the University of Calgary, were analyzed for comparison with the Quinn River samples (see footnote 1).

Organic Carbon Trends

The organic carbon curve shows multiple excursions between periods of apparent stability. The isotopic record shows a generally positive trend in the basal part of the unit 3 chert (Fig. 5), then a sharp negative excursion near the top of the unit. Values then trend back toward positive before another negative excursion is seen in the basal meters of unit 4. There is no distinct change in isotope values at the lithologic contact between units 3 and 4. The curve then stabilizes in the lower part of unit 4, before a positive excursion in the shaley middle part of the unit occurs. A sharp negative excursion occurs near the thin chert bed in the middle of unit 4, after which values remain relatively low until a positive excursion is seen near the top of the unit. Values become more negative at the base of unit 6, and the final two points trend back toward positive.

DISCUSSION

Depositional Environment of the Quinn River Formation

Tectonic, structural, and sedimentological evidence indicates that the Quinn River Formation was deposited near the flank of an island arc, perhaps in a backarc basin, where an apron of volcaniclastic debris interfingered with bathyal-abyssal biogenic sediments now represented by radiolarian and spicular chert. The presence of bedded radiolarian chert, the lack of observable trace fossils, and the turbiditic nature of volcaniclastic sandstones indicate that the strata record a deep-water (bathyal to abyssal) depositional environment.

Gravity-induced transport of some beds in the formation, particularly the granule to coarse-sand conglomerates in unit 6, would have resulted in substantial erosion of underlying sediments. However, aside from the thin cross-stratified volcaniclastic sandstone found ~2.5 m below the unit 3–unit 4 contact, there are no gravity flow deposits within the Permian–Triassic boundary interval. Although Wyld (1990) suggested the McCloud arc was undergoing uplift during Late Permian and Early Triassic times, the deep-water depositional setting of the Quinn River Formation would still have resulted in relatively uninterrupted bathyal-abyssal sedimentation during this period. The depositional setting, the lack of gravity flow deposits in the boundary interval, and the contiguous facies relationships throughout the section therefore suggest continuous deposition through the Permian–Triassic boundary on sedimentological grounds.

A useful lesson may be drawn from Permian–Triassic boundary strata in the Western Canada Sedimentary Basin (Henderson, 1997) and the Sverdrup Basin in Arctic Canada (Henderson and Baud, 1997). In these basins, the Permian–Triassic contact was previously considered unconformable and was placed at the lithologic change between the chert-rich Upper Permian formations (Ranger Canyon, Fantasque, Mowitch, and Degerbols–Van Hauen Formations) and the shaley Triassic formations (Sulphur Mountain, Grayling, Montney, and Blind Fiord Formations). However, detailed conodont biostratigraphy showed that many sections contain a complete Permian–Triassic succession. The condensed basal sediments of the transgressive black shales, previously assumed to be exclusively Triassic, contain uppermost Permian conodonts such as *Neogondolella rosenkrantzi, N. postbitteri, N. subcarinata,* and *N. meishanensis*. The Permian conodonts are conformably followed by earliest Triassic conodonts, including *Hindeodus parvus*. This is similar to the Japanese accreted terranes, where the Permian–Triassic boundary occurs not at the lithologic change but in the claystones following the shutdown of chert deposition (Isozaki, 1997). Thus, it is likely that the lowest shales and dolomicrites in unit 4 of the Quinn River Formation are condensed and of latest Permian age, with the actual Permian–Triassic boundary occurring in the basal meters of unit 4.

Placement of Stratigraphic Boundaries in the Quinn River Formation

One of the primary goals of this research has been to better identify detailed changes and subdivisions within the Quinn River Formation. Suggested correlations from the combination of biostratigraphy, isotope stratigraphy, and lithostratigraphy are presented as Figure 5. Most of the isotopic correlations were

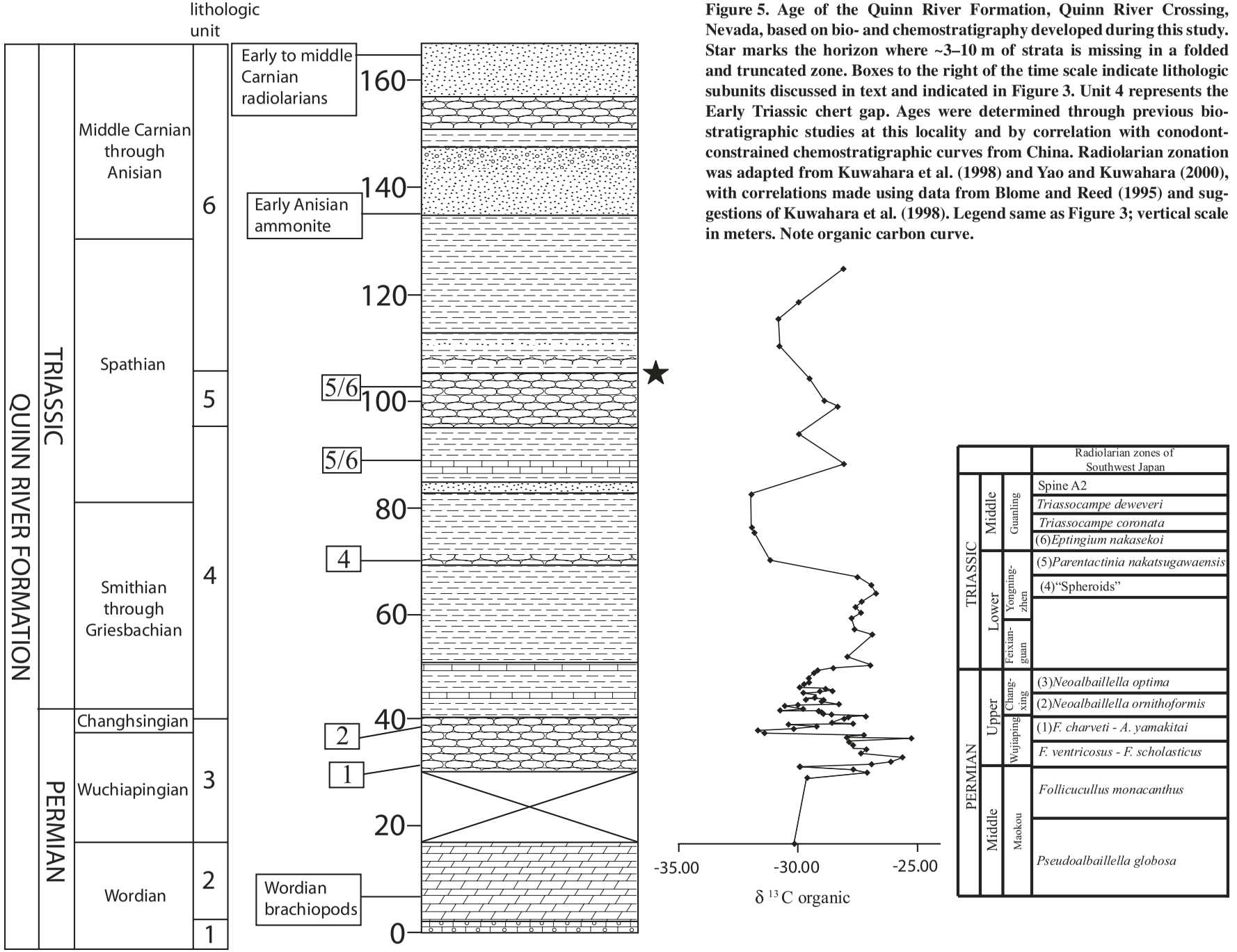

Figure 5. Age of the Quinn River Formation, Quinn River Crossing, Nevada, based on bio- and chemostratigraphy developed during this study. Star marks the horizon where ~3–10 m of strata is missing in a folded and truncated zone. Boxes to the right of the time scale indicate lithologic subunits discussed in text and indicated in Figure 3. Unit 4 represents the Early Triassic chert gap. Ages were determined through previous biostratigraphic studies at this locality and by correlation with conodont-constrained chemostratigraphic curves from China. Radiolarian zonation was adapted from Kuwahara et al. (1998) and Yao and Kuwahara (2000), with correlations made using data from Blome and Reed (1995) and suggestions of Kuwahara et al. (1998). Legend same as Figure 3; vertical scale in meters. Note organic carbon curve.

achieved by comparison with Payne et al.'s (2004) biostratigraphically calibrated curve for the Permian–Triassic interval. Although the Payne et al. (2004) curve analyzed inorganic carbon in limestone, variations in organic and inorganic carbon through the Permian–Triassic boundary interval display similar trends where both have been analyzed from the same section (Magaritz et al., 1992; Musashi et al., 2001; Sephton et al., 2002). Furthermore, whereas the degree of isotopic fractionation between organic and inorganic carbon changed slightly throughout this interval, causing difficulties for correlations based on magnitude, the two curves follow roughly similar tracks from the Cambrian through the Jurassic (Hayes et al., 1999). Owing to the continuous deep-water nature of the section, organic carbon provenance changes (e.g., Foster et al., 1998) are unlikely to have significantly affected the curve.

It should be noted that while sampling intensity in the vicinity of the Permian–Triassic boundary is relatively tight, samples from the upper part of the section are spaced at relatively long intervals (2–6 m). Given the constraints on isotope stratigraphy, it is apparent that the actual positions of the peaks and troughs of the curve could be different than those depicted in Figure 5 (Sperling and Phelps, 2005). Consequently, the isotopic correlations should be regarded as tentative and a best-guess estimate of the positions of boundaries between the known biostratigraphic datums provided by radiolarians and ammonites.

Wordian–Wuchiapingian Boundary

As suggested by Blome and Reed (1995), this boundary, placed at the lithologic contact between the Wordian dolomite (unit 2) and the overlying radiolarian chert (unit 3), represents a disconformity at which the Capitanian and lower Wuchiapingian are missing.

Wuchiapingian–Changhsingian Boundary

This boundary is placed at the change from the *F. charveti–A. yamakitai* Zone fauna to the *Neoalbaillella ornithoformis* Zone radiolarian fauna (Blome and Reed, 1995). The last appearance of albaillellids occurs ~7 m below the unit 3–unit 4 transition, and the first appearance of *N. ornithoformis* occurs ~3 m below the transition. A significant isotope excursion of $-4^{0/00}$ begins 3.7 m below the lithologic change, and it is suggested that this excursion may represent the one seen by Shao et al. (2000) between the Wujiaping and Changxing Formations in South China. It should be noted that these cherts contain very low TOC values (~0.06–0.10%), and this could be partly responsible for the extreme variability in the isotope values of unit 3.

Changhsingian–Griesbachian Boundary

The Changhsingian–Griesbachian boundary also represents the Permian–Triassic boundary, which is officially defined as the first appearance datum (FAD) of the conodont *Hindeodus parvus* in Meishan, China (Yin et al., 2001). Since few useful conodonts have been recovered from this section, the boundary is defined isotopically using the suggestion of Wignall et al. (1998), with the low point of the negative carbon isotope excursion representing the Permian–Triassic boundary. This negative excursion is seen worldwide in both inorganic (Baud et al., 1989; Jin et al., 2000) and organic carbon (Wang et al., 1994; Wignall et al., 1998) and represents a "truly useful marker for chemostratigraphic correlation in a global context" (Musashi et al., 2001). In the stratotype section, the Permian–Triassic boundary, as officially defined as the FAD of *H. parvus,* occurs slightly after the level of the mass extinction and negative carbon isotope excursion (Jin et al., 2000). Therefore, the Permian-Triassic boundary depicted in Figures 4 and 5 represents a level very high in the Changhsingian, probably near the mass extinction horizon, and not necessarily at the biostratigraphic boundary (see also Sperling and Phelps, 2005, for a further review of problems with isotopic correlations). The carbon isotope excursion suggested to mark the approximate Permian–Triassic boundary in the Quinn River Formation occurs 1.54 m above the base of the unit 4 dolomicrite-shale package and has a magnitude of $-3.61^{0/00}$. This is similar to the pattern seen in Permian–Triassic sequences at both Ursula Creek, British Columbia, and Opal Creek, Alberta (Henderson, 1997; Wignall and Newton, 2003), where chert deposition ceased in the Late Permian, and is followed within the next several meters by a significant negative organic carbon isotope excursion and the first appearance of *H. parvus*. Although no definitive fossils have been found in the base of unit 4 to unquestionably verify the age (and thereby remove the possibility of chemostratigraphic aliasing), the lithologic and biostratigraphic parallels to Canadian (Henderson, 1997) and Japanese (Isozaki, 1997) sections suggest that the excursion represents the approximate level of the boundary.

Smithian–Spathian Boundary

The lack of biostratigraphic data from unit 4 makes it difficult to confidently define the Griesbachian–Dienerian or the Dienerian–Smithian boundary. However, when the isotope stratigraphy is combined with the radiolarian biostratigraphy, it is possible to define the Smithian–Spathian boundary. The boundary should be somewhere between the "spheroid" zone (Lower Triassic, but likely Dienerian–Smithian) and the *P. nakatsugawaensis* (Spathian)–*H. gifuensis* (early Anisian) Zone–correlative radiolarians reported by Blome and Reed (1995).

It is suggested that the more positive isotopic values from meters 45–70 and the more negative values from meters 70–85 illustrated in Figure 5 correspond, respectively, to the Dienerian–Smithian isotopic high and the Smithian–Spathian isotopic low reported by Payne et al. (2004). The Smithian–Spathian boundary in the Quinn River Formation is therefore placed between the identified radiolarian zones near the isotopic low at 80 m in Figure 5. Similar to the Chinese sections, the Smithian negative excursion is also of high magnitude, representing a change of $-5.26^{0/00}$.

Spathian–Anisian Boundary

Blome and Reed (1995) report that radiolarian collections from this part of the section range through the Spathian (*P. nakatsugawaensis* Zone) and lower Anisian (*H. gifuensis* Zone). The next highest available biostratigraphic datum is the ammonite recovered by Jones (1990) and referred to as *Paracrochordiceras* by Blome and Reed (1995). The first appearance of this genus represents one of the "golden spikes" for the base of the Anisian (Gradstein et al., 2004). The occurrence of this ammonite ~40 m above the lowest occurrence of the *P. nakatsugawaensis–H. gifuensis*–correlative radiolarian faunas suggests that the radiolarian collections may be closer to Spathian age rather than Anisian.

The Spathian–Anisian boundary (corresponding to the boundary between the Lower and Middle Triassic) is placed between the occurrence of Spathian–Anisian radiolarians and the early Anisian ammonite. Further support for these correlations comes from the chemostratigraphic record; the isotopic high at ~90 m and the isotopic low at ~100 m in Figure 5 may correspond to the early Spathian high and the late Spathian low demonstrated by Payne et al. (2004).

The upper ~45 m of the Quinn River section therefore represents Anisian through early to middle Carnian sedimentation. This thickness represents considerably thinner strata than would be expected, given approximate sedimentation rates lower in the section. This is likely due to unconformities caused by fault contacts or the erosive power of coarse sand to granule conglomerates.

Redox Trends in the Late Permian–Early Triassic along the Western Pangean Margin

Permian Chert Event and the Early Triassic Chert Gap

Widespread deposition of biogenic chert marks the Middle and Upper Permian along the

western margin of Pangea (Murchey and Jones, 1992). Beauchamp and Baud (2002) dated the onset of the so-called Permian Chert Event at or near the Sakmarian–Artinskian boundary in the Sverdrup Basin of Arctic Canada, although deep-ocean chert deposition began earlier elsewhere (Isozaki, 1994). Beauchamp and Baud (2002) attributed the Permian Chert Event to northwestern Pangea having been bathed by cold waters derived from seasonal melting of northern sea ice. Other suggestions for these long-lived cherts include high nutrient concentrations from high-latitude upwelling (Kidder and Worsley, 2004) or large-scale volcano-hydrothermal activity during plate boundary reconfigurations (Racki and Cordey, 2000). Silica factories associated with the widespread deposition of radiolarian- and sponge spicule–rich sediments apparently shut down in the latest Permian, leading to the 8–10 Ma Early Triassic Chert Gap. Stratigraphic evidence (Beauchamp and Baud, 2002) indicates that this shutdown was rapid and resulted in a much warmer marine environment, consistent with modeling studies for the Late Permian (Kidder and Worsley, 2004; Kiehl and Shields, 2005).

Although the Early Triassic Chert Gap is no longer recognized as truly worldwide in extent (e.g., Takemura et al., 2003), it was nevertheless a widespread event. For example, the Jurassic accretionary complex in the Mino-Tamba belt of Japan shows a change from bedded chert to dark claystone and back to bedded chert across this interval (Isozaki, 1997). Ages obtained from the Permian and Triassic cherts at Quinn River correlate extremely well with the zenith, demise, and reappearance of chert, both along the Pangean margin (Beauchamp and Baud, 2002) and especially with accreted terranes in Japan (see Fig. 1 of Isozaki, 1997; the Early Triassic Chert Gap lasted from radiolarian zones P11 to T1 in both the Quinn River Formation and in Japan).

The existence of strong global controls on sedimentation at Quinn River is also supported by lithostratigraphic similarities of the accreted arc terrane at Quinn River and the continental-margin Ursula Creek section in British Columbia. In general, the similarities between Ursula Creek and Quinn River are striking despite their deposition in different basins. The Upper Permian Fantasque Formation at Ursula Creek consists of bedded radiolarian and spiculitic chert and shale. Radiolarians are abundant in these cherts, although the top 75 cm of the formation contains only small, chalcedony-filled spheres, which range into the lowermost dolomite beds 75 cm above the top of the chert. The Fantasque Formation at Urusla Creek is overlain by the Permian–Triassic Grayling Formation, the first 11 m of which consists of alternating shales and laminated, brown-weathering dolomicrites. The upper half of the Grayling Formation is mainly shaley, with the top of the formation being marked by the appearance of calcareous chert (Henderson, 1997; Wignall and Newton, 2003).

Quinn River and Ursula Creek show similar stratigraphic patterns, including the unusual dolomicrite beds deposited after the cessation of chert deposition. These dolomicrites look similar in thin section (GSA Data Repository Figs. DR1–DR12), and a geochemical discrimination diagram showing relative percentages of SiO_2, Al_2O_3, and CaO + MgO demonstrates the similarities in major element composition (Fig. 6). Both sections also show an increase in shale after an initial abundance of dolomicrites following the chert gap.

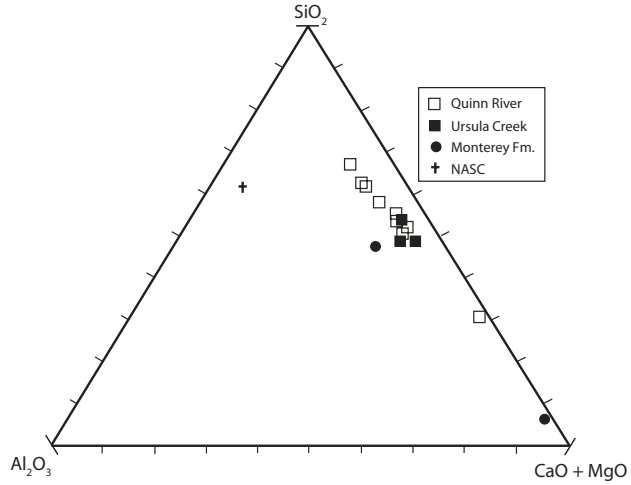

Figure 6. Geochemical comparison of dolomicrites—SiO_2, Al_2O_3 (the shale component) and CaO + MgO (the dolomite component)—in the Quinn River Formation, Nevada (open boxes) and the Grayling Formation, Ursula Creek section, British Columbia (closed boxes). Included for reference are the North American Shale Composite (cross) as described by Gromet et al. (1984) and two authigenic dolomite samples from the Miocene Monterey Formation, California (closed circles; Isaacs, 1992; Piper and Isaacs, 1995).

Redox Trends at Quinn River and Other Localities

In both the British Columbia and Nevada sections, the shutdown in chert deposition seems to be contiguous with evidence for the spread of dysoxic oceanic bottom waters. At Quinn River, the stratigraphically lower Permian cherts contain no evident pyrite, whereas the uppermost sample (QR-15) contains abundant cubic pyrite and is slightly darker in hand sample. The overlying dolomicrites and shales are well laminated and pyritic, and they contain relatively high levels of TOC (Fig. 7). Paleontological studies at Quinn River also support a decrease in oxygen levels near the top of unit 3. A study of sponge diversity at Quinn River shows that a diverse fauna at the base of the Permian chert was subsequently replaced by an exclusively hexactine fauna at the top of the unit, likely because of the spread of anoxic waters (Murchey, 1989; 2004, personal commun.). The reappearance of possible sponge spicules is seen in thin section in the Dienerian–Smithian(?) thin chert bed in unit 4, but true bedded chert does not reappear until unit 5.

A similar facies pattern, suggesting increasing anoxia toward the chert-shale lithologic boundary, is seen at Ursula Creek. The spiculitic cherts of the Fantasque Formation show pervasive bioturbation but are overlain by interbedded burrowed cherts and laminated pyritic cherts, and finally by laminated black shales and dolomicrites (Wignall and Twitchett, 2002; Wignall and Newton, 2003). Sponge spicules are common in the bioturbated beds of the uppermost 1 m of the Fantasque, but they are absent from the laminated beds, suggesting that redox levels controlled the sponges' colonization of the seafloor.

Trace metal studies from both sections complement the facies analysis and allow for finer resolution of paleo-redox conditions. Wignall and Twitchett (2002) found that the uppermost cherts at Urusla Creek became enriched in authigenic U (as shown by decreasing Th/U ratios measured by a field-portable gamma-ray spectrometer). A similar trend is seen in the trace-metal study at Quinn River. Trace-metal ratios for authigenic U and V/Cr suggesting oxic, dysoxic, and anoxic conditions (Jones and Manning, 1994) have been reproduced in Figure 7. Both of these ratios show a trend toward dysoxic

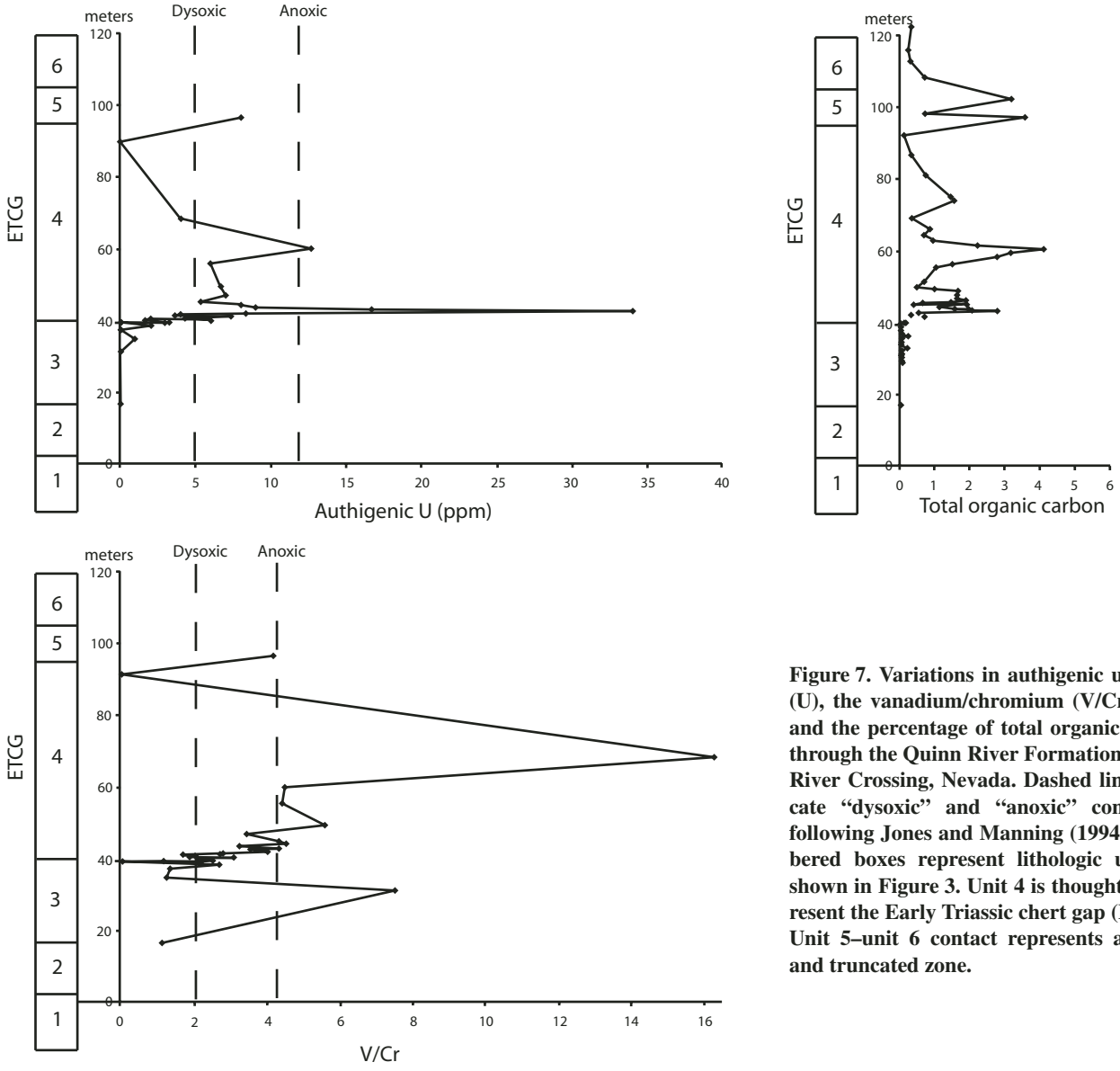

Figure 7. Variations in authigenic uranium (U), the vanadium/chromium (V/Cr) ratio, and the percentage of total organic carbon through the Quinn River Formation, Quinn River Crossing, Nevada. Dashed lines indicate "dysoxic" and "anoxic" conditions, following Jones and Manning (1994). Numbered boxes represent lithologic units as shown in Figure 3. Unit 4 is thought to represent the Early Triassic chert gap (ETCG). Unit 5–unit 6 contact represents a folded and truncated zone.

conditions around the lithologic change from bedded chert to dolomicrite/shales, with the initiation of the redox change having occurred during deposition of the chert (see Fig. 7).

Whereas trace metal or TOC variations between different lithologies (i.e., between chert and shale) cannot be reliably compared, the intra-lithologic changes in the chert should be comparable, at least in a relative sense. The uppermost thin chert beds (samples QR-15B and QR-15C) contain 3 and 1.66 ppm authigenic U, whereas the other chert samples (with the exception of QR-14A, which is also near the top of the unit) show essentially no authigenic U enrichment. The three uppermost cherts also contain about twice the TOC of the other chert samples. This indicates that the change toward more dysoxic conditions occurred during the latest Permian (approximately in the early Changhsingian on the basis of radiolarian biostratigraphy), coincident with deposition of the chert. While the trace metal parameters do not always agree for every sample in the section, the general pattern at Quinn River suggests that oxygen levels (1) decreased to dysoxic conditions around the chert-gap lithologic boundary, (2) declined to true anoxic conditions in the middle of the chert-gap strata, and (3) returned to more dysoxic-oxic conditions around the reappearance of chert. These results agree with geochemical studies of the Japanese sections, which show the development of long-lasting (10 m.y.) deep-water dysoxia-anoxia beginning in the Late Permian (Kato et al., 2002).

Noble and Renne (1990), in a combined study of the radiolarian and sponge faunas of the Permian–Triassic Dekkas and Pit Formations of the Eastern Klamath Terrane (also part of the McCloud arc), determined that the Upper Permian Dekkas cherts were deposited near a sponge biostrome in well-oxygenated bottom waters. Dekkas samples were hematitic and contained unbroken spicules and whole sponges. The overlying Pit Formation is marked by a basal gray-green chert containing Permian radiolarians (Silberling and Jones, 1982). The chert also contains small amounts of organic matter, euhedral pyrite, and only rare,

fragmented spicules. This chert is overlain by a thick, organic-rich (up to 2.7% TOC) shale containing framboidal pyrite indicative of dysoxic-anoxic deposition. Noble and Renne (1990) suggest that "it seems plausible that there was a partial closure of the basin to open oceanic circulation which stagnated the bottom water environment sufficiently to create anoxic conditions." More likely, the changes in redox state in the Pit Formation, and the decline of sponge and radiolarian communities in the Late Permian of the Eastern Klamath Terrane, were caused not by the tectonic movement of a basin sill but by the global or regional ocean stagnation that strongly affected the western Pangean margin (Isozaki, 1994, 1997; Wignall and Twitchett, 2002; Beauchamp and Baud, 2002; Kiehl and Shields, 2005). This same pattern is also seen in the continental-margin Opal Creek section, Alberta, where chert deposition ceased in the Late(?) Permian, and the cherty Ranger Canyon Formation is overlain (following a slight unconformity) by the black shales and dolomicrites of the Permian–Triassic Sulphur Mountain Formation (Henderson, 1997).

Because Quinn River, Ursula Creek, Opal Creek, and the Eastern Klamath Terrane, representing widespread environments ranging from continental margin to accreted arc terranes, show a change toward less oxic conditions near the Permian–Triassic chert-shale boundary, it is suggested that the Early Triassic Chert Gap was probably caused by ocean stagnation (as has been suggested by Wignall and Twitchett, 1996; Beauchamp and Baud, 2002) and the development of deep-water anoxia. Although a decrease in productivity may have affected input of biogenic silica from radiolarians to the sea-bottom sediment (as indicated by the Japanese sections; Isozaki, 1994), the spread of bathyal anoxic waters and its negative effect on benthic sponge communities was probably the most important factor in reducing chert deposition along the western Pangean margin. The fact that abundant radiolarian ghosts can be seen in thin section for several meters past the lithologic boundary indicates that the radiolarian communities were surviving in the more oxic surface layers of the water column, and that the main decrease in biogenic silica was due to loss of sponges.

Origin of Dolomicrites and Their Utility as Paleoenvironmental Indicators

The occurrence of early authigenic dolomicrites at Quinn River, Ursula Creek, Opal Creek, and perhaps elsewhere, is further indication of the broad oceanic controls that operated on marine sedimentation during Permian–Triassic time. Deep-water dolomites are a relatively unusual rock type, but they can be found forming in the modern ocean in bathyal continental-margin sediments containing >0.5% TOC and where sedimentation rates are <500 m/m.y. (Baker and Burns, 1985; Mazzullo, 2000). Analogous fossil deep-water dolomites have been reported from many Neogene organic-rich sediments, such as the Miocene Monterey Formation of California (Garrison, 1992; Garrison et al., 1994) and the Montana Member of the Gonfolite Lombarda Group, Italy (Bernoulli and Gunzenhauser, 2001). The Monterey Formation contains well-laminated, organic-rich deep-water dolomites interpreted to have been formed by precipitation within and beneath the zone of sulfate reduction.

Sulfate reduction, in which sulfate-reducing bacteria utilize SO_4 as an oxidant in a respiratory process that decomposes organic matter, is often expressed as

$$2CH_2O\ (\text{organic matter}) + SO_4^{2-} \rightarrow 2HCO_3^- + H_2S.$$

The early authigenic dolomite is formed as a result of the HCO_3^- from the sulfate reduction process combining with Ca^{2+} and Mg^{2+} that diffuses down from the water column (Burns et al., 2000; Mazzullo, 2000). This process also helps to limit the concentrations of SO_4^{2-}, which has been shown experimentally to reduce the degree of calcite dolomitization (Baker and Kastner, 1981). Garrison (1992) notes that, on the basis of the occurrence of disseminated dolomite at the sediment-water interface in diatomaceous sediments on the modern Peru margin and fully lithified dolomite layers 1.5 m below the seafloor, this zone of sulfate reduction occurs at or just beneath the seafloor in low-oxygen, organic-rich sediments. This Monterey-type model is favored for the formation of the Permian–Triassic dolomicrites on the western Pangean margin.

In thin section, extremely small dolomite rhombs can be seen replacing radiolarian ghosts in some dolomicrite beds of the Quinn River Formation, and the uppermost chert bed in the Fantasque Formation at Ursula Creek has dolomite rhombs partially replacing some of the chert. The formation of the facies F "transitional" rock at Quinn River, which is harder than associated shales but more friable than dolomicrites, is most easily explained by partial dolomitization, perhaps owing to more rapid burial that prevented diffusion of ions (Mazzullo, 2000). At Quinn River, the distribution of dolomicrite beds is generally negatively correlated with chert beds. Although cherty rocks briefly reappear at ~69 m (middle of unit 4), this bed is technically a radiolarian-bearing siliceous mudstone and not a true chert. This bed is also isolated and not part of a period of thick chert deposition as represented by unit 5. True bedded chert reappears in unit 5, at which point the dolomicrites disappear completely from the section. These cherts contain radiolarians ranging through the *P. nakatsugawaensis* Zone (~Spathian) or *H. gifuensis* Zone (early Anisian), the same time period when chert deposition resumed in the accreted terranes of Japan (Isozaki, 1997) and Thailand (Sashida et al., 2000). In general, the stratigraphic distribution of chert versus dolomicrite at Quinn River probably reflects changing paleo-redox conditions, with anoxic waters having a detrimental effect on siliceous sponge communities and encouraging the growth of sulfate-reducing bacteria that promoted the formation of early authigenic dolomite.

These distinctive dolomicrites may exist at other places along the former Pangean margin. The early authigenic dolomites are easily misidentified in the field as siltstones, as was originally the case for the Quinn River Formation. Many authors report brown-weathering siltstones and concretions in Lower Triassic strata, including the Lower–Middle Triassic Pit Formation of the Eastern Klamath Terrane (Miller, 1989), the Permian–Triassic Candelaria Formation in the Columbus Mining Area of Nevada (O'Connor, 2004), and the Lower Triassic Thaynes Formation of Idaho (Paull and Paull, 1991). Furthermore, Kakuwa (1996) reports thin dolostone interbeds directly above the chert gap in the Japanese accreted terranes, and dolomites (although perhaps not always Monterey-type dolomites as previously described) are a common feature in Permian–Triassic boundary sections worldwide (R. Twitchett, 2005, written commun.). Unusual and widespread lithologies appear to be a hallmark of the Lower Triassic (Pruss et al., 2005), and the recognition of other early authigenic dolomites formed during this time period will likely become more common in the future.

Although the links between the Permian–Triassic mass extinction and the development of deep-water anoxia that slightly but significantly preceded the extinction (Isozaki, 1997; Kato et al., 2002; this study) are not yet fully understood, widespread microbial sulfate reduction encouraged by anoxic bottom waters, of which the early authigenic dolomites are the sedimentologic evidence, would have helped increase concentrations of H_2S in the water column. This may have created oceanic conditions similar to those of the mid-Proterozoic, where the surface waters were oxygenated, but the deep ocean was anoxic and sulfidic (Anbar and Knoll, 2002). The subsequent incursion of this H_2S onto the shelf or into the atmosphere could possibly represent a kill mechanism for the Permian–Triassic extinction (Kump et al., 2005; Grice et al., 2005).

CONCLUSIONS

The Permian–Triassic Quinn River Formation represents deep-water (bathyal to abyssal) sedimentation adjacent to a continent-fringing arc system. The section was previously believed to be incomplete because of facies relationships between bedded chert and an overlying "siltstone," as well as a lack of latest Permian and earliest Triassic fossils. This study demonstrates that the siltstone is in fact a radiolarian-bearing dolomicrite, indicating contiguous deep-water facies relationships with the chert. The dolomicrites most likely formed by early authigenic precipitation in a low-oxygen setting within organic-rich sediments, just beneath the sediment-water interface. Similar dolomicrites can be found in other localities worldwide, following cessation of chert deposition in the latest Permian. Their widespread occurrence indicates that broad regional or global oceanic controls, specifically stagnation and the development of dysoxic to anoxic bottom water, controlled the distinctive lithostratigraphic patterns along the margin. Trace metal studies complement the facies analysis and confirm the existence of widespread and long-lasting deep-water anoxia-dysoxia through the latest Permian and Early Triassic.

New radiolarian zonations indicate that the uppermost Permian chert in the Quinn River Formation is early Changhsingian in age. The "spheroid" radiolarian zone (Lower Triassic) was discovered ~29 m above the stratigraphically-highest Permian chert. Organic carbon isotope stratigraphy, in conjunction with previous biostratigraphic studies, assists in the delineation of the Permian–Triassic, Smithian–Spathian, and Spathian–Anisian boundaries. Because of general problems with chemostratigraphic correlation, these boundaries must be regarded as tentative. Nonetheless, the combined evidence suggests relatively continuous slow sedimentation on the bathyal seafloor through the Permian–Triassic boundary at Quinn River. This interpretation stands in contrast to the previous simple downward extrapolation of Middle Triassic fossil ages to the lithologic boundary between Quinn River Formation units 3 and 4. This is similar to patterns reported from the Western Canada Sedimentary Basin and from Japan, where the Permian–Triassic boundary is found in the basal meters of a black shale overlying cherts and not at the distinct lithologic boundary. Whereas enhanced biostratigraphy in the Lower Triassic portion of the Quinn River Formation is necessary for more detailed studies of the Permian–Triassic extinction, the Quinn River Formation exposed in the Bilk Creek Mountains, Nevada, probably represents a complete Permian–Triassic section.

Finally, the Quinn River Formation organic carbon isotopic record demonstrates patterns of variation similar to those recorded by Payne et al. (2004) from the eastern margin of the Panthalassic superocean. Whether or not the shifts are synchronous, multiple positive and negative excursions of 3–5‰ were found in the Quinn River Formation, supporting the Payne et al. (2004) suggestion that the Permian–Triassic isotope excursion was not an isolated event.

ACKNOWLEDGMENTS

This project was made possible by Paleontological Society Grants-in-aid and grants from the Stanford McGee fund to E.A.S. S. Graham, P. Wignall, Y. Isozaki, and an anonymous reviewer provided constructive reviews of an earlier version of this manuscript. Feedback from W. Alvarez, T. Beatty, E. Crafford, G. Garrison, R. Garrison, C. Henderson, D. Lowe, B. Murchey, D. O'Connor, J. Payne, A. Paytan, and P. Ward was also helpful. We thank M. Balsley, A. Abeles, and B. Romans for field assistance, and T. Teague and D. Mucciarone for laboratory assistance.

REFERENCES CITED

Alvarez, W., and O'Connor, D., 2002, Permian–Triassic boundary in the southwestern United States: Hiatus or continuity?, *in* Koeberl, C., and MacLeod, K.G., eds., Catastrophic events and mass extinctions: Impacts and beyond: Geological Society of America Special Paper 356, p. 385–393.

Anbar, A.D., and Knoll, A.H., 2002, Proterozoic ocean chemistry and evolution: A bioinorganic bridge?: Science, v. 297, p. 1137–1142, doi: 10.1126/science.1069651.

Baker, P.A., and Burns, S.J., 1985, Occurrence and formation of dolomite in organic-rich continental margin sediments: American Association of Petroleum Geologists Bulletin, v. 69, p. 1917–1930.

Baker, P.A., and Kastner, M., 1981, Constraints on the formation of sedimentary dolomite: Science, v. 213, p. 214–216.

Baud, A., Magaritz, M., and Holser, W.T., 1989, Permian–Triassic of the Tethys: Carbon isotope studies: Geologische Rundschau, v. 78, p. 649–677, doi: 10.1007/BF01776196.

Beauchamp, B., and Baud, A., 2002, Growth and demise of Permian biogenic chert along northwest Pangea: Evidence for end-Permian collapse of thermohaline circulation: Palaeogeography, Palaeoclimatology, Palaeoecology, v. 184, p. 37–63, doi: 10.1016/S0031-0182(02)00245-6.

Becker, L., Poreda, R.J., Hunt, A.G., Bunch, T.E., and Rampino, M., 2001, Impact event at the Permian–Triassic boundary: Evidence from extraterrestrial noble gas in fullerenes: Science, v. 291, p. 1530–1533, doi: 10.1126/science.1057243.

Benton, M.J., and Twitchett, R.J., 2003, How to kill (almost) all life: The end-Permian extinction event: Trends in Ecology & Evolution, v. 18, p. 358–365, doi: 10.1016/S0169-5347(03)00093-4.

Bernoulli, D., and Gunzenhauser, B., 2001, A dolomitized diatomite in an Oligocene–Miocene deep-sea fan succession, Gonfolite Lombarda Group, Northern Italy: Sedimentary Geology, v. 139, p. 71–91, doi: 10.1016/S0037-0738(00)00159-7.

Blome, C., and Reed, K., 1992, Permian and Early(?) Triassic radiolarian faunas from the Grindstone Terrane, central Oregon: Journal of Paleontology, v. 66, p. 351–383.

Blome, C., and Reed, K., 1995, Radiolarian biostratigraphy of the Quinn River Formation, Black Rock terrane, north-central Nevada: Correlations with eastern Klamath terrane geology: Micropaleontology, v. 41, p. 49–68.

Bowring, A., Erwin, D.H., Jin, Y.G., Martin, M.W., Davidek, K., and Wang, W., 1998, U/Pb zircon geochronology and tempo of the end-Permian mass extinction: Science, v. 280, p. 1039–1045, doi: 10.1126/science.280.5366.1039.

Burns, S.J., McKenzie, J.A., and Vasconcelos, C., 2000, Dolomite formation and biogeochemical cycles in the Phanerozoic: Sedimentology, v. 47, supp. 1, p. 49–61, doi: 10.1046/j.1365-3091.2000.00004.x.

Collinson, J.W., Kendall, C.G., and Marcental, J.B., 1976, Permian–Triassic boundary in eastern Nevada and west-central Utah: Geological Society of America Bulletin, v. 87, p. 821–824, doi: 10.1130/0016-7606(1976)87<821:PBIENA>2.0.CO;2.

Erwin, D.H., Bowring, S.A., and Yugan, J., 2002, End-Permian mass extinctions: A review, *in* Koeberl, C., and MacLeod, K.G., eds., Catastrophic events and mass extinctions: Impacts and beyond: Geological Society of America Special Paper 356, p. 363–383.

Feng, Q., and Gu, S., 2002, Uppermost Changxingian (Permian) radiolarian fauna from Southern Guizhou, Southwestern China: Journal of Paleontology, v. 76, p. 797–809.

Foster, C.B., Logan, G.A., and Summons, R.E., 1998, The Permian–Triassic boundary in Australia: Where is it and how is it expressed?: Proceedings of the Royal Society of Victoria, v. 110, p. 247–266.

Garrison, R.E., 1992, Neogene lithofacies and depositional sequences associated with upwelling regions along the eastern margin of the Pacific, *in* Tsuchi, R., and Ingle, J.C., eds., Pacific Neogene: Tokyo, University of Tokyo Press, p. 43–68.

Garrison, R.E., Hoppie, B.W., and Grimm, K.A., 1994, Phosphates and dolomites in coastal upwelling sediments of the Peru margin and the Monterey Formation (Naples Beach Section), California, *in* Hornafius, J.S., ed., Field guide to the Monterey Formation between Santa Barbara and Gaviota, California: Pacific Section, American Association of Petroleum Geologists, v. GB72, p. 67–84.

Gradstein, F.M., Ogg, J.G., Smith, A.G., Bleeker, W., and Lourens, L.J., 2004, A new geologic time scale, with special reference to Precambrian and Neogene: Episodes, v. 27, p. 83–100.

Grice, K., Cao, C., Love, G.D., Bottcher, M.E., Twitchett, R.J., Grosjean, E., Summons, R.E., Turgeo, S.C., Dunning, W., and Jin, Y., 2005, Photic zone euxinia during the Permian–Triassic superanoxic event: Science, v. 307, p. 706–709, doi: 10.1126/science.1104323.

Gromet, L.P., Dymek, R.F., Haskin, L.A., and Korotev, R.L., 1984, The "North American Shale Composite": Its compilation, major and trace element characteristics: Geochimica et Cosmochimica Acta, v. 48, p. 2469–2482, doi: 10.1016/0016-7037(84)90298-9.

Hayes, J.M., Strauss, H., and Kaufman, A.J., 1999, The abundance of ^{13}C in marine organic matter and isotopic fractionation in the global geochemical cycle of carbon during the past 800 Ma: Chemical Geology, v. 161, p. 103–125, doi: 10.1016/S0009-2541(99)00083-2.

Hein, J.R., 2004, The Permian earth, *in* Hein, J.R., ed., Life cycle of the Phosphoria Formation: From deposition to post-mining environment: Amsterdam, Elsevier, p. 3–17.

Henderson, C.M., 1997, Uppermost Permian conodonts and the Permian–Triassic boundary in the Western Canada Sedimentary Basin: Bulletin of Canadian Petroleum Geology, v. 45, p. 693–707.

Henderson, C.M., and Baud, A., 1997, Correlation of the Permian–Triassic boundary in Arctic Canada and comparison with Meishan, China: Proceedings of the 30th International Geological Congress, v. 11, p. 143–152.

Isaacs, C.M., 1992, Preliminary data on rock samples (KG-1 to KG-24) in the Cooperative Monterey Organic Geochemistry Study, Santa Maria and Santa Barbara–Ventura Basins, California: U.S. Geological Survey Open-File Report 92-539-C, 29 p.

Ishiga, H., 1986, Late Carboniferous and Permian radiolarian biostratigraphy of Southwest Japan: Journal of Geosciences, Osaka City University, v. 29, p. 89–100.

Isozaki, Y., 1994, Superanoxia across the Permo-Triassic boundary: Record in accreted deep-sea pelagic chert in Japan: Canadian Society of Petroleum Geologists Memoir 17, p. 805–812.

Isozaki, Y., 1997, Permo–Triassic boundary superanoxia and stratified superocean: Records from lost deep

sea: Science, v. 276, p. 235–238, doi: 10.1126/science.276.5310.235.
Jin, Y., Wang, Y., Wang, W., Shang, Q.H., Cao, C.Q., and Erwin, D.H., 2000, Pattern of marine mass extinction near the Permian–Triassic boundary in South China: Science, v. 289, p. 432–436, doi: 10.1126/science.289.5478.432.
Jones, A.E., 1990, Geology and tectonic significance of terranes near Quinn River Crossing, Nevada, *in* Harwood, D.S., and Miller, M.M., eds., Paleozoic and early Mesozoic paleogeographic relations: Sierra Nevada, Klamath Mountains, and related terranes: Geological Society of America Special Paper 255, p. 239–253.
Jones, B., and Manning, D.A.C., 1994, Comparison of geochemical indices used for the interpretation of palaeoredox conditions in ancient mudstones: Chemical Geology, v. 111, p. 111–129, doi: 10.1016/0009-2541(94)90085-X.
Kaiho, K., Kujiwara, Y., Nakano, T., Miura, Y., Kuwahata, H., Tazaki, K., Ueshima, M., Chen, Z.Q., and Shi, G.R., 2001, End-Permian catastrophe by a bolide impact: Evidence of a gigantic release of sulfur from the mantle: Geology, v. 29, p. 815–818, doi: 10.1130/0091-7613(2001)029<0815:EPCBAB>2.0.CO;2.
Kakuwa, Y., 1996, Permian-Triassic mass extinction event recorded in bedded chert sequence in southwest Japan: Palaeogeography, Palaeoclimatology, Palaeoecology, v. 121, p. 35–51.
Kato, Y., Nakao, K., and Isozaki, Y., 2002, Geochemistry of Late Permian to Early Triassic pelagic cherts from southwest Japan: Implications for an oceanic redox change: Chemical Geology, v. 182, p. 15–34, doi: 10.1016/S0009-2541(01)00273-X.
Ketner, K.B., and Wardlaw, B.R., 1981, Permian and Triassic rocks near Quinn River Crossing, Humboldt County, Nevada: Geology, v. 9, p. 123–126, doi: 10.1130/0091-7613(1981)9<123:PATRNQ>2.0.CO;2.
Kidder, D.L., and Worsley, T.R., 2004, Causes and consequences of extreme Permo–Triassic warming to globally equable climate and relation to the Permo–Triassic extinction and recovery: Palaeogeography, Palaeoclimatology, Palaeoecology, v. 203, p. 207–237, doi: 10.1016/S0031-0182(03)00667-9.
Kiehl, J.T., and Shields, C.A., 2005, Climate simulations of the Latest Permian: Implications for mass extinction: Geology, v. 33, p. 757–760, doi: 10.1130/G21654.1.
Knoll, A.H., Bambach, R.K., Canfield, D.E., and Grotzinger, J.P., 1996, Comparative earth history and Late Permian mass extinction: Science, v. 273, p. 452–457.
Kozur, H.W., 1998, Some aspects of the Permian–Triassic boundary (PTB) and of the possible causes for the biotic crisis around this boundary: Palaeogeography, Palaeoclimatology, Palaeoecology, v. 143, p. 227–272, doi: 10.1016/S0031-0182(98)00113-8.
Kump, L.R., Pavlov, A., and Arthur, M.A., 2005, Massive release of hydrogen sulfide to the surface ocean and atmosphere during intervals of oceanic anoxia: Geology, v. 33, p. 397–400, doi: 10.1130/G21295.1.
Kuwahara, K., Yao, A., and Yamakita, S., 1998, Reexamination of Upper Permian radiolarian biostratigraphy: Earth Science, v. 52, p. 391–404.
Magaritz, M., Krishnamurthy, R.V., and Holser, W.T., 1992, Parallel trends in organic and inorganic carbon isotopes across the Permian/Triassic boundary: American Journal of Science, v. 292, p. 727–739.
Mazzullo, S.J., 2000, Organogenic dolomitization in peritidal to deep-sea sediments: Journal of Sedimentary Research, v. 70, p. 10–23.
McDaniel, S.B., 1982, Permian–Triassic source bed analysis at Quinn River Crossing, Humboldt County, Nevada [M.S. thesis]: Reno, University of Nevada, 120 p.
Miller, E.L., Miller, M.M., Stevens, C.H., Wright, J.E., and Madrid, R., 1992, Late Paleozoic paleogeographic and tectonic evolution of the western U.S. Cordillera, *in* Burchfiel, B.C., et al., eds., The Cordilleran Orogen: Conterminous U.S.: Boulder, Colorado, Geological Society of America, The Geology of North America, v. G-3, p. 57–106.
Miller, M.M., 1987, Dispersed remnants of a northeast Pacific fringing arc: Upper Paleozoic terranes of Permian McCloud faunal affinity, Western U.S.: Tectonics, v. 6, p. 807–830.
Miller, M.M., 1989, Intra-arc sedimentation and tectonism: Late Paleozoic evolution of the eastern Klamath terrane, California: Geological Society of America Bulletin, v. 101, p. 1063–1076.
Murchey, B.L., 1989, Late Paleozoic siliceous basins of the western Cordillera of North America (Nevada, California, Mexico, and Alaska)—Three studies using radiolarians and sponge spicules for biostratigraphic, paleobathymetric and tectonic analysis [Ph.D. thesis]: Santa Cruz, University of California, 187 p.
Murchey, B.L., and Jones, D.L., 1992, A mid-Permian chert event—Widespread deposition of biogenic siliceous sediments in coastal, island arc and oceanic basins: Palaeogeography, Palaeoclimatology, Palaeoecology, v. 96, p. 161–174, doi: 10.1016/0031-0182(92)90066-E.
Musashi, M., Isozaki, Y., Koike, T., and Kreulen, R., 2001, Stable carbon isotope signature in mid-Panthalassa shallow-water carbonates across the Permo-Triassic boundary: Evidence for ^{13}C-depleted superocean: Earth and Planetary Science Letters, v. 191, p. 9–20, doi: 10.1016/S0012-821X(01)00398-3.
Noble, P., and Renne, P., 1990, Paleoenvironmental and biostratigraphic significance of siliceous microfossils of the Permo–Triassic Redding Section, Eastern Klamath Mountains, California: Marine Micropaleontology, v. 15, p. 379–391, doi: 10.1016/0377-8398(90)90021-D.
O'Connor, D., 2004, The Permian–Triassic boundary in the Great Basin, western USA [Ph.D. thesis]: Berkeley, University of California, 335 p.
Paull, R.A., and Paull, R.K., 1991, Allochthonous rocks from the western part of the Early Triassic miogeocline: Hawley Creek area, east-central Idaho: Contributions to Geology, University of Wyoming, v. 28, p. 145–154.
Payne, J.L., Lehrmann, D.J., Wei, J., Orchard, M.J., Schrag, D.P., and Knoll, A.H., 2004, Large perturbations of the carbon cycle during recovery from the End-Permian extinction: Science, v. 305, p. 506–509, doi: 10.1126/science.1097023.
Piper, D.Z., and Isaacs, C.M., 1995, Geochemistry of minor elements in the Monterey Formation, California: Seawater chemistry of deposition: U.S. Geological Survey Professional Paper 1566, 41 p.
Pruss, S.B., Corsetti, F.A., and Bottjer, D.J., 2005, The unusual sedimentary rock record of the Early Triassic: A case study from the southwestern United States: Palaeogeography, Palaeoclimatology, Palaeoecology, v. 222, p. 33–52, doi: 10.1016/j.palaeo.2005.03.007.
Racki, G., and Cordey, F., 2000, Radiolarian palaeoecology and radiolarites: Is the present the key to the past?: Earth-Science Reviews, v. 52, p. 83–120, doi: 10.1016/S0012-8252(00)00024-6.
Raup, D.M., and Sepkoski, J.J., 1982, Mass extinctions in the marine fossil record: Science, v. 215, p. 1501–1503.
Renne, P.R., Zhang, Z., Richards, M.A., Black, M.T., and Basu, A.R., 1995, Synchrony and causal relations between Permian–Triassic boundary crises and Siberian flood volcanism: Science, v. 269, p. 1413–1416.
Sashida, K., 1997, Radiolarian biostratigraphy near the Permian–Triassic boundary: Circular Society Science Form, v. 12, p. 30.
Sashida, K., Hisayoshi, I., Adachi, S., Ueno, K., Kajiwara, Y., Nakornsri, N., and Sarsud, A., 2000, Late Permian to Middle Triassic radiolarian faunas from Northern Thailand: Journal of Paleontology, v. 74, p. 789–811.
Sephton, M.A., Looy, C.V., Veefkind, R.J., Brinkhuis, H., de Leeuw, J.W., and Visscher, H., 2002, Synchronous record of δ^{13}C in the oceans and atmosphere at the end of the Permian, *in* Koeberl, C., and MacLeod, K.G., eds., Catastrophic events and mass extinctions: Impacts and beyond: Geological Society of America Special Paper 356, p. 455–462.
Shao, L., Zhang, P., Dou, J., and Shen, S., 2000, Carbon isotope compositions of the late Permian carbonate rocks in southern China: Their variations between the Wujiaping and Changxing formations: Palaeogeography, Palaeoclimatology, Palaeoecology, v. 161, p. 179–192, doi: 10.1016/S0031-0182(00)00122-X.
Silberling, N.J., and Jones, D.L., 1982, Tectonic significance of Permian–Triassic strata in northwestern Nevada and northern California: Geological Society of America Abstracts with Programs, v. 14, p. 234.
Skinner, J.W., and Wilde, G.L., 1966, Permian fusulinids from northwestern Nevada: University of Kansas Paleontological Contributions Paper, v. 4, part 1, p. 1–10.
Sperling, E.A., and Phelps, N.K., 2005, The efficacy of carbon isotope stratigraphy for identifying and correlating the Permian–Triassic boundary: Geological Society of America Abstracts with Programs, v. 37, no. 7, p. 160.
Sugiyama, K., 1992, Lower and Middle Triassic radiolarians from Mt. Kinkazan, Gifu Prefecture, central Japan: Transactions and Proceedings of the Palaeontological Society of Japan, new series, v. 167, p. 1180–1223.
Takemura, A., Aita, Y., Sakai, T., Kamata, Y., Szuki, N., Hori, R.S., Yamakita, S., Sakakibara, M., Campbell, H.J., Fujiki, T., Ogane, K., Takemura, S., Sakamoto, S., Kodama, K., and Nakamura, Y., 2003, Conodont-based age determinations for a radiolarian-bearing Lower Triassic chert sequence in Arrow Rocks, New Zealand: Tenth Meeting of the International Association of Radiolarian Paleontologists Abstracts and Programme, p. 108.
Wang, K., Geldsetzer, H.H.J., and Krouse, H.R., 1994, Permian–Triassic extinction: Organic δ^{13}C evidence from British Columbia, Canada: Geology, v. 22, p. 580–584, doi: 10.1130/0091-7613(1994)022<0580:PTEOCE>2.3.CO;2.
Wignall, P.B., and Newton, R., 2003, Contrasting deep-water records from the Upper Permian and Lower Triassic of South Tibet and British Columbia: Evidence for a diachronous mass extinction: Palaios, v. 18, p. 153–167.
Wignall, P.B., and Newton, R., 2004, Reply—Contrasting deep-water records from the Upper Permian and Lower Triassic of South Tibet and British Columbia: Evidence for a diachronous mass extinction: Palaios, v. 19, p. 102–104.
Wignall, P.B., and Twitchett, R.J., 1996, Oceanic anoxia and the end-Permian mass extinction: Science, v. 272, p. 1155–1158.
Wignall, P.B., and Twitchett, R.J., 2002, Extent, duration and nature of the Permian–Triassic superanoxic event, *in* Koeberl, C., and MacLeod, K.G., eds., Catastrophic events and mass extinctions: Impacts and beyond: Geological Society of America Special Paper 356, p. 395–413.
Wignall, P.B., Morante, R., and Newton, R., 1998, The Permo–Triassic transition in Spitsbergen: $\delta^{13}C_{org}$ chemostratigraphy, Fe and S geochemistry, facies, fauna and trace fossils: Geological Magazine, v. 135, p. 47–62, doi: 10.1017/S0016756897008121.
Willden, R., 1961, Major westward thrusting of post–Middle Triassic age in northwestern Nevada, *in* Shorter papers in the geologic and hydrologic sciences, Articles 147–292, Geological Survey Research: U.S. Geological Survey Professional Paper 424-C, p. C116–C120.
Wyld, S.J., 1990, Paleozoic and Mesozoic rocks of the Pine Forest Range, northwest Nevada, and their relation to volcanic arc assemblages of the western U.S. Cordillera, *in* Harwood, D.S., and Miller, M.M., eds., Paleozoic and early Mesozoic paleogeographic relations; Sierra Nevada, Klamath Mountains, and related terranes: Geological Society of America Special Paper 255, p. 219–237.
Yao, A., and Kuwahara, K., 2000, Permian and Triassic radiolarians from the southern Guizhou Province, China: Journal of Geosciences, Osaka City University, v. 43, p. 1–19.
Yin, H., Zhang, K., Tong, J., Yang, Z., and Wu, S., 2001, The Global Stratotype Section and Point (GSSP) of the Permian–Triassic boundary: Episodes, v. 24, p. 102–114.

Manuscript Received by the Society 4 February 2005
Revised Manuscript Received 14 September 2005
Manuscript Accepted 17 November 2005

Printed in the USA